

Structural determination of Co/TiO₂ nanocomposite: XRD technique and simulation analysis

F. MOSTAGHNI^{1,*}, Y. ABED²

¹Chemistry Department, Payam Noor University, Iran

²Physic Department, Payam Noor University, Iran

Synthesis and complex theoretical and experimental studies of Co/TiO₂ anatase have been reported. The preparation of Co/TiO₂ was carried out by sol-gel method. Distribution of cations among the two tetrahedral and octahedral sites was estimated by analyzing the powder X-ray diffraction patterns by employing Rietveld refinement technique, and the results revealed the existence of tetragonal structure. Band structure and density of states calculations were performed using the first-principles methods. The structural and electronic properties of Co/TiO₂ were calculated in the general gradient approximation (GGA). An additional comparison with pure TiO₂ anatase allowed us to clarify cobalt doping effect on the electronic structure and the band gap. The band gap of Co/TiO₂ was decreased by broadening the valence band as a result of the overlap among Co 3d, Ti 3d, and O 2p states, which made it respond better to visible and solar light.

Keywords: *Rietveld refinement; XRD; band structure; density of states; metal doping TiO₂*

© Wrocław University of Technology.

1. Introduction

TiO₂ has been widely used as semiconductor because of its high oxidative power, chemical stability, low cost and nontoxicity [1–3]. One of the most important properties of semiconductor nanoparticles (NPs) is their capability to generate electrons and holes after absorbing photon with energy equal to or greater than their gap energy. However, as a wide band gap oxide semiconductor ($E_g = 3.23$ eV), anatase TiO₂ only shows photocatalytic activity under UV-light irradiation ($\lambda < 384$ nm) which accounts for merely (ca. 5 %) of total solar spectrum [4, 5].

Doping of TiO₂ by low amounts of foreign elements including transition metals, such as V [6], Mo [7], Fe [8–10], Co [11, 12], Pt [13], Au [14], Cr [15], Nd [16] is currently attracting considerable interest as a promising route to improve TiO₂ photocatalytic performance under visible-light irradiation [17–19]. Some experimental results [20, 21] have revealed that co-doping TiO₂ could narrow

its band gap, thereby increasing the efficiency of the photocatalysis in the visible range. Co-doped anatase, in particular, is an object of a very large number of publications and review papers [22–29]. Amadelli et al. [30] synthesized cobalt-modified TiO₂ by the incipient impregnation method. They found that the modified oxide presents higher photoactivity both under illumination with UV-Vis ($\lambda > 360$ nm) and visible light ($\lambda > 420$ nm; $\lambda > 450$ nm), and that this enhancement depends on the amount of added species and on the final thermal treatment in the preparation step.

Doping of semiconductors changes the probability for charge carriers to participate in conduction. In order to quantify this probability we need the density of states (DOS) within the semiconductor as a function of electron energy. The density of states combined with the probability distribution of states at a particular energy to be occupied provide the overall density of charge carriers as a function of energy [31].

Therefore, the understanding of detailed electronic structure of semiconductors has been a challenging problem in electronics. Unfortunately,

*E-mail: mostaghni@yahoo.com

measurements of structure and electronic properties of crystals require a specified laboratory, as well as excellent quality materials, which is generally expensive. In contrast to experimental investigations, a theoretical analysis by computer simulations could overcome the effects of complex experimental factors and clarify the ion doping effects on crystal and electronic structure.

Quantum chemistry calculations for modifying the band gap of TiO₂ have been reported, including studies on transition metals co-doping of TiO₂ photocatalysts [32–45]. Yalc et al. [46] performed calculations based on density functional theory (DFT) to characterize the influence of Fe³⁺ doping on the electronic and structural properties of TiO₂. Recently, first-principles calculations were conducted for Fe-doped TiO₂ [47–49].

Liu et al. [50] calculated the crystal structure, band gap, density of states and optical absorption coefficient of pure anatase TiO₂ and cobalt doped anatase TiO₂ by a plane-wave ultrasoft pseudopotential method based on the density functional theory of the first-principles.

In our previous study [51] we carried out a systematic analysis of cobalt impurity states at different concentrations as well as their influence on the TiO₂ band structure and density of states using GGA with CASTEP code. The results showed that the band gap is greatly sensitive to the dopant concentration. It has been observed that higher concentration of cobalt enhances conductivity of TiO₂. It is important to note that at a moderate level of doping (20 %) the lowest band gap occurs. Further increase in dopant concentration up to 25 % results in larger band gap. Therefore, the best concentration of cobalt dopant was 20 % based on the first-principles calculations.

In this study, we have reported the synthesis of Co/TiO₂ anatase (20 %) and theoretical analysis which was performed by Rietveld X-ray diffraction. In the Rietveld analysis, we fit a model to the data. If the model is correct, then it shall predict the structure and electronic properties of the nanocomposites. The results were discussed for undoped and Co-doped TiO₂ nanoparticles (NPs) and conclusions were drawn from the results.

2. Material and methods

2.1. Synthesis of Co/TiO₂

All chemicals used in the experiments were of analytical reagent grade. Co/TiO₂ nanopowders were prepared via sol-gel method using the precursor titanium isopropoxide (TTIP, 97 %, Sigma Aldrich), cobalt nitrate, polyethylene glycol (average molecular weight: 4000), deionized water and methanol as the starting materials. In a typical experiment, 20 mL of methanol was added to 24.06 g of TTIP to yield a light yellow solution. The mixture solution was stirred for 30 min using magnetic stirrer. Then, 5 mL methanol and 3.5 mL acetic acid glacial was added and stirred for 1 h at room temperature. For doping purpose, 25 mmol of Co(NO₃)₂·6H₂O (6.227 g) and 1 g PEG were dissolved in 10 mL of a solution of methanol: H₂O (1:1) to yield a light red solution. Two liquids were mixed and stirred for 1 h to produce a gel of bluish-purple color. After aging for 24 h, the gel was dried at room temperature and then it was dried at 60 °C for 2 h and calcined at 450 °C for 3 h.

Crystal structure of Co/TiO₂ nanoparticles was determined with a Bruker diffractometer, CuKα X-ray of wavelength ($\lambda = 1.5406 \text{ \AA}$). The XRD patterns were recorded in the 2θ range of 10° to 90° with a step width of 0.02 s⁻¹. The optical properties of the anatase Co/TiO₂ were characterized using UV-Vis diffuse reflectance spectroscopy.

2.2. Simulation analysis

The Accelrys Materials Studio 5.5 visualization package was used to create the TiO₂ nanoparticles of the anatase phase. The X-ray diffraction (XRD) pattern was analyzed with the help of reflex module by employing Rietveld refinement technique. The XRD pattern of Co/TiO₂ was refined using the 141/amd space group [52]. The CASTEP module was employed to calculate the structural, electronic, and optical properties of two samples. Generalized gradient approximation (GGA) with the Perdew-Burke-Ernzerhof was used for all calculations.

3. Results and discussion

3.1. X-ray diffraction studies

The X-ray diffraction pattern of the Co doped TiO₂ nanoparticles treated at 450 °C is shown in Fig. 1. The crystalline phase of the sample is predominantly anatase with the absence of secondary or impurity peaks. The XRD pattern exhibits strong diffraction peaks at 25.25°, 37.76°, 48.00°, 54.38° and 62.83° indicating TiO₂ in anatase phase.

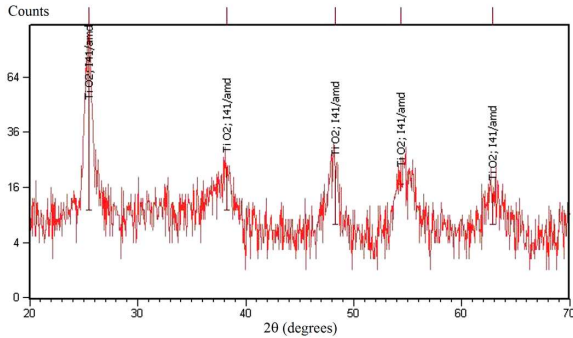


Fig. 1. Powder XRD pattern of the Co/TiO₂ anatase.

The crystalline size of the particles in the anatase phase was calculated using the modified Debye-Scherrer equation [53]. The modified Scherrer equation plot $\ln \beta$ against $\ln 1/\cos \theta$ has an intercept of the least squares line regression $\ln k\lambda/L$. After getting the intercept, the exponent of the intercept is obtained:

$$e^{\ln \frac{k\lambda}{L}} = \frac{k\lambda}{L} \quad (1)$$

Having $k = 0.9$ and λ ($\lambda_{\text{CuK}\alpha} = 0.15405$ nm), a single value of L is obtained for all of the available peaks. The results indicate that nanocrystalline Co/TiO₂ powder with crystallite size of 11 nm has been successfully obtained.

3.2. Rietveld analysis

The Rietveld method is a well-established technique for extracting structural details from powder diffraction data [54]. This method is based on a least-squares fit between step-scan data of a measured diffraction pattern and a simulated

X-ray-diffraction pattern. In this study, the crystalline structure of the Co/TiO₂ anatase was analyzed in detail by Rietveld profile refinement method in reflex module. The XRD patterns for these samples have refined using the 141/amd space group (Fig. 2).

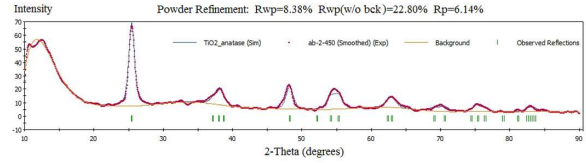


Fig. 2. Rietveld plot obtained by using the true instrumental function.

The fitting quality of the experimental data was assessed by computing the parameters R-pattern factor R_p and the weighted-profile factor R_{wp} [55, 56]. These factors are defined as:

$$R_{wp} = \left[\frac{\sum_i (I_o - I_c)^2 w_i}{\sum_i I_o^2 w_i} \right]^2 \quad (2)$$

$$R_p = \frac{\sum_i |y_{io} - y_{ic}|}{\sum_i y_{io}} \quad (3)$$

I_o and I_c are the observed and calculated integrated Bragg intensities, respectively (without background). The structural properties and R values for the sample annealed at 450 °C have been listed in Table 1.

Table 1. The structural properties and profile R values for the anatase phase.

u ^e	v	w	R _{wp}	R _p
0.34741	0.20303	-0.05045	8.38	6.14

The calculated R factors indicates that the calculated and experimental diffraction patterns match, therefore the model may represent the original sample.

3.3. Electronic properties

All calculations were performed with the CASTEP module using the first-principle calculations. The electronic structures and band parameters for pure anatase TiO₂ and Co/TiO₂ were obtained within the GGA approximations. The energy

band structure and density of states (DOS) of pure TiO₂ are shown in Fig. 3.

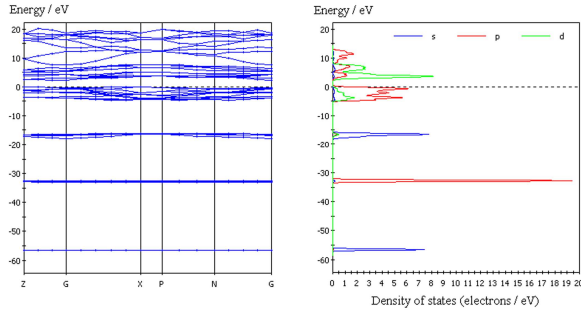


Fig. 3. Calculated band structures and partial density of states of pure TiO₂.

The band structure of pure anatase TiO₂ shows semiconducting behavior because in this case direct energy band gap is 2.29 eV. As shown in Fig. 3, it is less than the experimental value $E_g = 3.23$ eV due to the limitation of the generalized-gradient approximation (GGA). The energy zero represents the valence-band maximum. The composition of the calculated band gaps can be deduced from the density of states (Fig. 3). The conduction band, consists mainly of 4d titanium states, with a contribution of 3p states of oxygen. The dominating states in the valence band come from 3d states of titanium and 2p states of oxygen. These two states are strongly mixed with each other.

Then, we used GGA method in the Co doped TiO₂ band structure and density of state calculations. The results are given in the Fig. 4. In fact, the DOS shape of Co ions doping has become smoother and broader than that of pure TiO₂.

Co-doped TiO₂ shows more conducting behavior because there are many bands crossing the Fermi level. In this case, the indirect energy band gap is 1.59 eV (Fig. 4). These energy bands are mainly from the 3d states of cobalt and titanium and 2p states of oxygen around the Fermi energy. In fact, an impurity level appears between valence band and conduction band, reducing the band gap. The dominating contribution to the conductivity originally comes from the 3p states of oxygen.

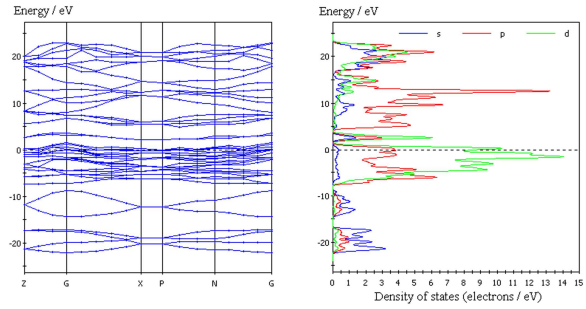


Fig. 4. Calculated band structures and partial density of states of Co/TiO₂.

3.4. Optical bandgap

The optical absorption spectra were recorded on Shimadzu UV-Vis-NIR-3100 spectrophotometer in the wavelength range of 200 nm to 800 nm at room temperature. Fig. 5 shows UV-Vis absorption spectrum of Co/TiO₂ nanoparticles.

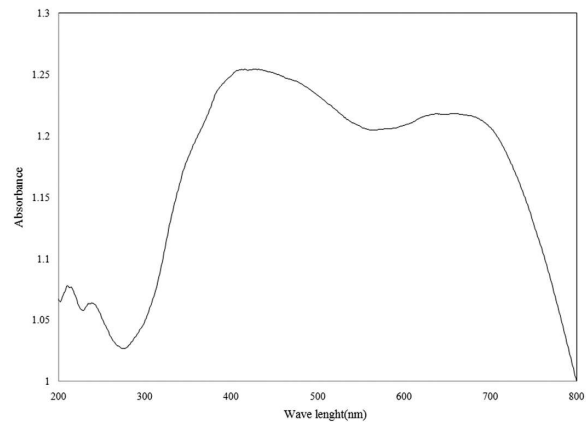


Fig. 5. UV-Vis absorption spectrum of the Co/TiO₂.

The exciton absorption is at about 477 nm. The band gap energy has been determined using the Tauc's relation [57] which is given by:

$$(\alpha h\nu)^{\frac{1}{2}} = A (h\nu - E_g) \quad (4)$$

where α is absorption coefficient, $h\nu$ is energy of photon, E_g is optical band gap and A is a transition probability constant. Fig. 6 shows the curve $(\alpha h\nu)^{1/2}$ versus $h\nu$ for cobalt doped TiO₂. By extrapolating the linear part of this curve we have obtained the indirect bandgap 1.64 eV, which is

smaller than 3.08 reported for pure TiO₂ [58]. The cobalt doped (colored) sample also absorbs light in the visible region around 1.64 eV (red light) in agreement with the sample being green.

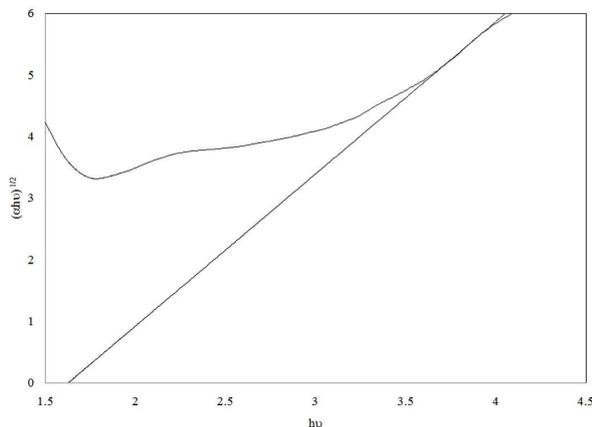


Fig. 6. Plot $(\alpha hv)^{1/2}$ vs. photon energy.

4. Conclusions

In this study, Co/TiO₂ nanocrystals were produced using sol-gel method. Rietveld refinement of XRD data for the samples was performed. The obtained results show a good conformity between the observed X-ray diffraction pattern and that calculated by Rietveld method. The optimization was carried out according to R_p and R_{wp} . The best agreement between the calculated and observed data was obtained for tetragonal structures. In addition, anatase TiO₂ doping with cobalt can effectively narrow the band gap as a result of the overlap among the 3d states of Co, Ti, and 2p states of oxygen, which enhances photocatalytic activity in the visible light region. Both the broadening of the valence band and cobalt impurity states within the band gap might also enhance the photocatalytic activity.

Acknowledgements

We would like to show our gratitude to the Payam Noor University for their support and encouragements.

References

- [1] COLMENARES J.C., ARAMENDIA M.A., MARINAS A., MARINAS J.M., URBANO F.J., *Appl. Catal. A*, 306 (2006), 120.
- [2] CRISAN M., BRAILEANU A., RAILEANU M., ZAHARESCU M., CRISAN D., DRAGAN N., ANASTASESCU M., IANCULESCU A., NITOI I., MARINESCU V.E., HODOROGEA S.M., *J. Non-Cryst. Solids*, 354 (2008), 705.
- [3] DING X., AN T., LI G., ZHANG S., CHEN J., YUAN J., ZHAO H., CHEN H., SHENG G., FU J., *J. Colloid Interf. Sci.*, 320 (2008), 501.
- [4] WANG X., MENG S., ZHANG X., WANG H., ZHONG W., DU Q., *Chem. Phys. Lett.*, 444 (2007), 292.
- [5] KATO H., KUDO A., *J. Phys. Chem. B*, 106 (2002), 5029.
- [6] TSUYUMOTO I., NAWA K., *J. Mater. Sci.*, 43 (2008), 985.
- [7] DU Y.K., GAN Y.Q., YANG P., ZHAO F., HUA N.P., JIANG L., *Thin Solid Films*, 491 (2005), 133.
- [8] YAMASHITA H., HARADA M., MISAKA J., TAKEUCHI M., NEPPOLIAN B., ANPO M., *Catal. Today*, 84 (2003), 191.
- [9] ZHU S., SHI T., LIU W., *Physica B*, 396 (2007), 177.
- [10] NAEEM K., OUYANG F., *Physica B*, 405 (2010), 221.
- [11] SUBRAMANIAN M., VIJVALAKSHMI S., VENKATARAJ S., JAVAVEL R., *Thin Solid Films*, 516 (2008), 3776.
- [12] SARKAR D., GHOSH C.K., MAITI U.N., CHATTOPADHYAY K.K., *Physica B*, 406 (2011), 1429.
- [13] WENBIN X., SSHURONG D., DEMIAO W., GAOCHAO R., *Physica B*, 403 (2008), 2698.
- [14] ZHOU M., ZHANG J., CHENG B., YU H., *Int. J. Photoenergy*, 2012 (2012), 532843.
- [15] SSLMA W., SAFIA A., LUNNA M., ANUM D., FAROOQ B., REHANA Z., *Mater. Sci.-Poland*, 33 (2015), 508.
- [16] MAZUR M., KACZMAREK D., DOMARADZKI J., WOJCIESZAK D., MAZUR P., PROCIOW E., *Mater. Sci.-Poland*, 31 (2013), 71.
- [17] CARP O., HUISMAN C.L., RELLER A., *Prog. Solid State Ch.*, 32 (2004), 33.
- [18] ANPO M., *B. Chem. Soc. Jpn.*, 77 (2004), 1427.
- [19] MOHAMED R.M., MCKINNEY D.L., SINGMUND W.M., *Mater. Sci. Eng. R-Rep.*, 73 (2012), 1.
- [20] WENG W., MA M., DU P., *Surf. Coat. Tech.*, 198 (2005), 340.
- [21] NACEUR J.B., MECHIAKH R., BOUSBIH F., CHTOUROU R., *Appl. Surf. Sci.*, 257 (2011), 10699.
- [22] MATSUMOTO Y., MURAKAMI M., SHONO T., *Science*, 291 (2001), 854.
- [23] SULLIVAN J.M., ERWIN S.C., *Phys. Rev. B*, 67 (2003), 144415.
- [24] PRELLIER W., FFOUCHET A., MERCEY B., *J. Phys.-Condens. Mat.*, 15 (2003), 1583.
- [25] GENG W.T., KIM K.S., *Solid State Commun.*, 129 (2004), 741.
- [26] BRYAN J.D., HEALD S.M., CHAMBERS S.A., GAMELIN D.R., *J. Am. Chem. Soc.*, 126 (2004), 11640.
- [27] SIMPSON J.R., DREW H.D., SHINDE S.R., CHOUDHARY R.J., OGAL S.B., VENKATESAN T., *Phys. Rev. B*, 69 (2004), 193205.

- [28] COEY J.M.D., *Mater. Sci.*, 10 (2006), 83.
- [29] JANISCH R., SPALDIN N.A., *Phys. Rev. B*, 73 (2006), 035201.
- [30] AMADELLI R., SAMIOLO L., MALDOTTI A., MOLINARI A., VALIGI M., GAZZOLI D., *Int. J. Photoenergy*, 2008, 853753.
- [31] JING L.Q., SUN X.J., XIN B.F., WANG B.Q., CAI W.M., FU H.G., *J. Solid State Chem.*, 77 (2004), 3375.
- [32] ZHENG S., GUOHAO W., ZHANG G., SUOLIANG Z., JIE S., LEI L., FANG W., RUI Z., XIAOBING Y., *Mater. Sci.-Poland*, 32 (2014), 93.
- [33] HONGPING L., LIN C., SHUAI L., CHANGSHENG L., JIAN M., ZHONGCHANG W., *Mater. Sci.-Poland*, 33 (2015), 549.
- [34] BARDZINSKI P., *Mater. Sci.-Poland*, 29 (2011), 223.
- [35] MAEDA K., DOMEN K., *J. Phys. Chem. C*, 111 (2007), 7851.
- [36] YOON J., SHIM E., JOO H., *J. Chem. Eng. Data*, 26 (2009), 1296.
- [37] CHEN X., SAMUEL S., *J. Chem. Rev.*, 107 (2007), 2891.
- [38] LU X.M., XIE J.M., YIN CH Q., *J. Chinese Ceram. Soc.*, 35 (2007), 983.
- [39] MIN S.P., KWON S.K., MIN I., *J. Phys. Rev. B*, 65 (2002), 1.
- [40] SHI J.Y., LENG W.H., CAO J.L., *J. Chem. Phys.*, 19 (2006), 463.
- [41] KARTHIK K., KESAVA PANDIAN S., SURESH KUMAR K., *J. Appl. Surf. Sci.*, 256 (2010), 4757.
- [42] IWASAKI M., HARA M., KAWADA H., *J. Colloid Interf. Sci.*, 224 (2000), 202.
- [43] SUBRAMANIAN M., VIJAYALAKSHMI S., VENKATARAJ S., *Thin Solid Films*, 516 (2008), 776.
- [44] AMADELLI R., SAMIOLO L., MALDOTTI A., *Int. J. Photoenergy*, 2008 (2008), 1.
- [45] ZHAO Z.Y., LIU Q.J., ZHANG J., *J. Chinese Phys. Soc.*, 56 (2007), 6592.
- [46] YALC Y., KILIC M., INAR Z.C., *Appl. Catal. B- Environ.*, 99 (2010), 469.
- [47] HOU X., HUANG M., WU X., LIU A., *Sci. China G*, 52 (2009), 838.
- [48] SU Y., XIAO Y., LI Y., DU Y., ZHANG Y., *Mater. Chem. Phys.*, 126 (2011), 761.
- [49] JIA L., WU C., HAN S., *J. Alloy. Compd.*, 509 (2011), 6067.
- [50] LIU H., SUN X., SUN M., ZHANG Y. XUE B., LIU Y., *J. Chinese Ceram. Soc.*, 39 (2011), 1617.
- [51] MOSTAGHNI F., ABED Y., *Phys. Chem. Chem. Phys.*, 5 (2015), 34.
- [52] PAN G., JING W., QING L., WENFANCHIN Z., *Physica B*, 19 (2010), 087103.
- [53] MONSHI A., FOROUGHI M.R., MONSHI M.R., *World Nano Sci. Eng.*, 2 (2012), 154.
- [54] POLVAKOV N.E., LESHINA T.V., METELEVA E.S., DUSHKIN A.V., KONOVALOVA T.A., KISPERS L.D., *J. Phys. Chem. B*, 114 (2010), 14200.
- [55] YOUNG R.A., *Introduction to the Rietveld Method: The Rietveld Method*, Oxford University Press, Oxford, 1993.
- [56] TOBY B.H., *Powder Diffr.*, 21 (2006), 67.
- [57] SONMEZOGLU S., ÇANKAYA G., SERIN N., *Mater. Technol.*, 27 (2012), 251.
- [58] KERNAZHITSKY L., SHYMANOVSKA V., GAVRILKO T., NAUMOV V., KSHNYAKIN V., *Ukr. J. Phys. Opt.*, 14 (2013), 15.

Received 2015-10-03
Accepted 2016-05-30